MAPPING FIRE AND FIREFIGHTER VISIBILITY FOR IMPROVING SITUATIONAL AWARENESS

by

Katherine Ann Mistick

A thesis submitted to the faculty of
The University of Utah
in partial fulfillment of the requirements for the degree of

Master of Science

Department of Geography

The University of Utah

May 2022

The University of Utah Graduate School

STATEMENT OF THESIS APPROVAL

The thesis of **Katherine Ann Mistick**

has been approved by the following supervisory committee members:

Philip E. Dennison	, Chair	**4/11/2022** Date Approved
Alexander Hohl	, Member	**4/11/2022** Date Approved
Michael James Campbell	, Member	**4/11/2022** Date Approved

and by **Philip E. Dennison** , Chair/Dean of the Department/College/ School of **Geography**

and by David B. Kieda, Dean of The Graduate School.

ABSTRACT

Wildland firefighters assume exceptional risk while mitigating the hazards wildfires pose to life and property. While certain protocols and safety initiatives have been developed to improve wildland firefighters' situational awareness, research has not yet focused on quantifying and mapping visibility that wildland firefighters possess surrounding an active wildfire. A major component of situational awareness during a wildland fire event is maintaining a line of sight with the fire and with the crew. This research seeks to compare methods for determining visibility at the scale of a wildland fire event, including fire visibility and crew visibility. In a wildland environment, visibility is dictated by terrain and vegetation. For this reason, two elevation models (a terrain model representing bare-earth and a surface model inclusive of vegetation) are considered. Further, owing to the fact that the precision of these models affects the accuracy of visibility estimation, two spatial resolutions (1 m and 30 m) are considered. The Green Ridge fire – ignited July 7th, 2021, in southeastern Washington, USA – serves as the case study for this research. Crew and fire visibility is calculated for each date, elevation model, and spatial resolution. Visibility across all dates is considered in aggregate and comparisons between elevation model and resolution are made using median regression. Results of these comparisons reveal that bare-earth elevation and 30 m models overestimate visibility by up to 29% and 94%, respectively. The most realistic model, based on a 1 m digital surface model, produced the most limited average

percentage of visible area (8.32%, crew; 11.38 %, fire). Overlapping visibility, or areas on the landscape with a view of both crew and fire hazard, are most limited spatially (with an average of 0.34 km^2), suggesting few areas exist providing good visibility of both crew and fire hazards. The results show that more spatially-precise landscape models provide necessary detail for determining visibility surrounding an active wildfire but are still limited by generalizations and significant processing times.

TABLE OF CONTENTS

LIST OF TABLES

Tables

LIST OF FIGURES

Figures

ACKNOWLEDGMENTS

I would like to thank my advisor and committee chair, Dr. Phil Dennison, for his expertise and mentoring throughout my graduate career at the University of Utah. Without his balanced, methodical approach to mentoring, this project would not have found such success. I would also like to thank Dr. Mickey Campbell for his mentoring, especially with the twists and turns of working with lidar data. I would also like to thank Dr. Alexander Hohl for completing my supervisory committee and for providing a necessary perspective.

In addition to my committee members, I would like to thank the National Interagency Fire Center, and Andrew Lacey of the Forest Service for providing me with data critical to this project. Thank you to Matt Thompson and Nate Anderson of the Forest Service for their feedback as this project was developed.

Finally, I would like to thank my family and friends for their continued support of my academic pursuits.

CHAPTER 1

INTRODUCTION

As wildfires increase in frequency, size, and intensity (Abatzoglou et al., 2021; Balch et al., 2018; Dennison et al., 2014a; Westerling et al., 2006), wildland firefighters are exposed to increased risk as they attempt to suppress such fires. Firefighting is inherently dangerous. In order to mitigate safety risk, many initiatives have been developed to understand and address the causes of firefighter fatalities (Page et al., 2019; National Wildfire Coordinating Group, 2017). One of the top five causes of firefighter fatalities is entrapment, when one or more firefighters becomes trapped by fire. While vehicle or stress-related incidents may be more common, entrapments have the potential to injure or kill multiple firefighters in a single incident, as was the case of the Yarnell Hill fire where 19 firefighters tragically lost their lives (Arizona State Forestry Division, 2013). Despite a long-term decrease in firefighter deaths from entrapment, multiple-fatality entrapment incidents remain a risk to firefighter safety (NWCG, 2017).

One key protocol developed to improve firefighter safety is Lookouts, Communications, Escape Routes, and Safety Zones (LCES) introduced by Gleason (1991). Lookouts are experienced wildland firefighters assigned to specifically monitor changes – such as weather, fire behavior, and crew movement – that are indicative of potential hazards (Gleason, 1991). Communication(s) stresses the importance of direct

and prompt contact between firefighters and incident management. Escape routes are predefined paths to safety, of which there must be multiple options (NWCG 2022; Gleason 1991). Lastly, safety zones are predefined areas of refuge should fire behavior introduce unsafe conditions for firefighting or escape (NWCG 2022, Beighley 1995).

At its core, LCES seeks to highlight and improve situational awareness for wildland firefighters. Situational awareness, or one's dynamic perception of their surroundings, has been studied in detail for high-risk, constantly changing situations such as those found in the military (Baek et al., 2018; Nofi, 2000), medical field (Gillespie et al., 2013; Graafland et al., 2014), and firefighting (Jolly & Freeborn, 2017; Page & Butler, 2018). Not only does situational awareness encompass the ability to perceive one's current situation, it also incorporates one's ability to predict and respond to changes in a manner that best supports one's desired outcome (Stanton et al., 2001). In the case of wildland firefighting, this means constantly monitoring and reevaluating the environment, hazard, and safety frameworks such as LCES in order to minimize risk to life and property. However, understanding and evaluating situational awareness is more straightforward than maintaining it in an active fire situation, which becomes difficult owing to several factors including fire behavior, firefighter qualifications and experience, topography, and human factors like organization and psychology (Mangan, 2001; Page & Butler, 2018).

Recent research has focused on improving firefighter safety by increasing our understanding of one or more aspects of situational awareness, as it pertains to wildland firefighting. Jolly & Freeborn 2017 developed a framework for determining fire behavior risk rating to improve situational awareness, while other studies have focused on

uncovering the effects of topography and fuel on entrapment potential (Lahaye, 2018; Page & Butler 2018; Page 2019). Another area of research has focused on geospatial modeling of escape routes and safety zones, aiming to improve our understanding of travel rates (Campbell et al., 2019a; Campbell et al., 2019b; Campbell et al., 2017a; Sullivan et al., 2020) and spatial attributes of safety zones (Campbell et al., 2022; Campbell, 2017b; Dennison et al., 2014b). While many of these studies have covered critical aspects of LCES, one aspect that has gone largely unexamined is the importance of lookouts and their responsibility to maintain a line of sight to both crew and fire hazards. Gleason (1991), however, does not limit the importance of sight to just lookouts. He states that any firefighter has the authority to alert others of perceived threats. Currently, wildland firefighters rely on training and experience, as well as communication with fire management, to best position themselves on the landscape where visiblity of both fire and other crew is maximized. This demonstrates the importance of studying and mapping lines of sight, or visibility, to improve situational awareness for wildland firefighters.

The objective of this study is to examine the tradeoffs between different data sources and methods for mapping visibility surrounding active portions of a fire in order to maximize a wildland firefighter's visibility of both fire hazard and crew location. Improving our understanding of the strengths and limitations of different data sources and methods for visibility mapping could provide a foundation for potential future operational use. For example, given an active fire perimeter or a prediction of future fire spread, this analysis could be conducted in real time to provide a map of relative visibility to fire crews, enabling them to manage the fire from locations that will maximize situational

awareness. It also has the potential to provide insight into the optimal placement of lookouts.

CHAPTER 2

BACKGROUND

In the United States, the importance of early detection and suppression of wildfires gained significant attention following the Great Fire of 1910 (Egan, 2009). As early as 1905 manned mountaintops with cabins were used to detect wildfires, and eventually, manned towers were common throughout forests in the United States (Grosvenor, 1999). Towers continued to be used throughout most of the 20th century, but innovative technology such as remote sensing and machine learning (Barmpoutis et al., 2020) have made staffed fire towers nearly obsolete, landing many on the National Register of Historic Places. Methods commonly used today include remotely operated cameras, aerial vehicles, or satellites (Kinaneva et al., 2019; Schroeder et al., 2014).

While much visibility research focuses on early fire detection from these new methods (Allison et al., 2016; Barmpoutis et al., 2020; Yuan et al., 2015), not much research has been devoted to Qua. This perspective is critical to account for when attempting to improve firefighter safety. Typically, on-the-ground visibility is quantified through a viewshed or line-of-sight (LOS) calculation. These types of analyses determine what is and is not visible on a landscape from one or more observation locations (Figure 1).

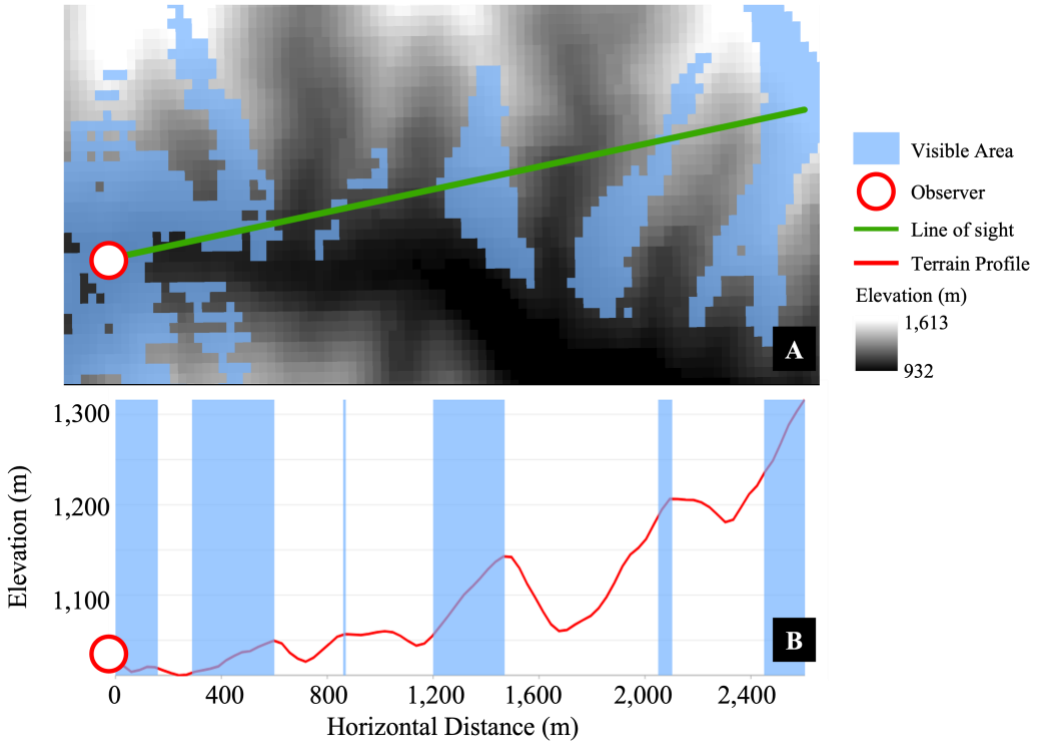

Figure 1. Viewshed schematic. **(A)** Map of elevation overlaid with viewshed results indicating visible pixels (blue) calculated from the observer. Green line indicates a single line of sight. **(B)** Aligned terrain profile of line of sight (red line) with guides indicating visible areas.

A viewshed is calculated as the sum of all possible lines of sight from a given perspective, accounting for any obstructions between the observer and a pre-defined maximum distance of interest. It is possible to calculate viewsheds assuming a flat plane or accounting for the Earth's curvature using geodesic methods. If no intermediate obstructions are present in the entire line of sight, the target would be considered visible. If any intermediate obstruction (e.g., an elevation above the line of sight) is present, the target will not be visible (Figure 1). Viewsheds have been used across disciplines including archeology, landscape and urban planning, social sciences, and environmental science (Bartie et al., 2011; Yu et al., 2016; Chamberlain & Meitner, 2013; Fisher et al.,

1997; Murgoitio et al., 2013; Vukomanovic et al., 2018). While previous research has shown the usefulness of viewshed algorithms in applications across fields, their use in wildland firefighter safety has yet to be explored.

While viewshed calculations provide a straightforward method for determining visibility– the state of and/or degree to which something can be seen – on a landscape, there are assumptions that come with mapping visibility based on a rasterized elevation model. Visibility can easily be overestimated according to the spatial resolution of the analysis surface (Vukomanovic et al., 2018). For example, when using 30 m spatial resolution data the calculation assumes that the entire 900 m^2 pixel is either visible or invisible. This assumption can be remedied with higher spatial resolution data, if available. However, these data usually involve tradeoffs such as larger file sizes, increased processing time/power, and limited coverage. Further, when using a terrain model as the analysis surface we assume no other obstructions exist, which is a faulty assumption to make in areas with an abundance of above-ground surface features, such as trees in a forest or buildings in an urban setting (Bartie et al., 2011; Murgoitio et al., 2013). Previous work has tried to address these concerns using advanced algorithms (Dean, 1997; Llobera, 2007) to account for vegetation obstructions. More recent work has focused on incorporating more detailed surfaces into viewshed calculations using lidar data (Doneus et al., 2022; Gargoum & Karsten, 2021; Lecigne et al., 2020; Murgoitio et al., 2013; Vukomanovic et al., 2018). Lidar – light detection and ranging –is an active remote sensing technique that uses a pulsed laser to capture precise above-ground elevation points (Lefsky et al., 2002). These data are captured in a point cloud format, with the density of data dictating the amount of detail captured (Lefsky et al.,

2002).

Using a surface model that includes vegetation or an algorithm to account for through-stand visibility may address certain assumptions made when calculating visibility. However, there are a variety of tradeoffs when determining visibility according to different input data that need to be explicitly quantified. Bartie et al. (2011) determined a combined approach was useful for urban visibility, using a bare earth terrain model along with a surface model to incorporate building height, and a vegetation map to include partial visibility through urban trees. However, their application focused solely on urban visibility. Murgoitio et al. 2013 studied through-stand visibility in lodgepole pine in Central Idaho, a landscape that is prone to wildland fire (National Park Service, 2021). However, visibility analyses pertaining specifically to wildland firefighters working active fires have not been investigated.

Specifically characterizing visibility in an active fire landscape is important as it is a much more complex and dynamic environment than previous studies have considered. Unlike stationary targets, wildland fire moves across the landscape in semi-predictable ways (Alexander & Cruz, 2006; Pastor et al., 2003; Salis et al., 2016). Wildland fires span a large range of spatial scales, ranging from a few hectares to many km^2 in size. While Vukomanovic et al. 2018 considered visibility over long distances (10 km radius), their focus was on stationary objects (residences). Other prior visibility studies have been more limited in spatial scale (e.g. 60 m in Murgoitio et al., 2013, up to 2.8 km in Gargoum & Karsten, 2021, and <250 m in Bartie et al., 2011). Beyond the spatial scale and dynamic nature of wildland fire, crews are not stationary and are frequently moving through the environment, making assessment of visibility over space

particularly important. This research is unique in assessing visibility for both firefighting crews and wildland fire over space using a variety of different geospatial inputs.

CHAPTER 3

METHODS

3.1 Study Area

The Green Ridge fire in southeastern Washington, USA (Figure 2) was ignited by lightning on July 7th, 2021, and served as the case study for this analysis. Growing to over 174 km^2, this fire had nearly 400 assigned personnel during peak fire activity (InciWeb, 2021). Bare-earth elevation in the immediate vicinity of the fire ranges from approximately 924 meters to 1,942 meters.

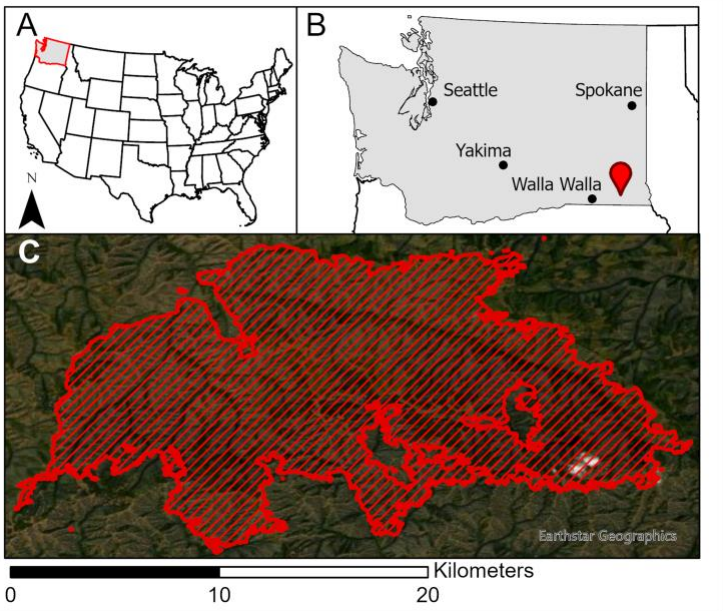

Figure 2. Green Ridge fire location. **(A)** Washington, USA. **(B)** Red pin indicates the fire location in southeastern Washington. **(C)** Cross-hatched area indicates one of the last infrared-captured fire perimeters for the Green Ridge fire, on September 12th, 2021.

The landscape is tree-dominated primarily with a closed canopy. LANDFIRE classifies most of the area as a mixed conifer forest including Douglas fir, ponderosa pine, and lodgepole pine. Vegetation heights range from <1 meter up to 38 meters. A few open-canopy and deciduous shrub-dominated areas exist within the immediate vicinity of the fire as well.

3.2 Elevation Models

Two types of digital elevation models (DEMs) were compared in this study: digital terrain models (DTMs), where pixel values represent the mean elevation of the terrain, absent any aboveground features (Figure 3B, D), and digital surface models (DSMs), where pixel values represent the elevation of the terrain and aboveground features (Figure 3A, C). Both models were considered at fine-scale resolution (1 m; Figure 3A, B) and coarse-scale resolution (30 m) (Figure 3C, D). Fine-scale elevation models were derived from USGS 3DEP airborne lidar, acquired between fall of 2017 and summer of 2018 and published for use in 2019 (USGS, 2019). The average point density of this dataset is 8.06 pts/m^2, and the entire final Green Ridge fire perimeter and surrounding landscape is captured by this product. Default point cloud classifications allowed me to generate a 1 m DTM using ground points and a 1 m DSM using first-return points to incorporate vegetation heights. All lidar processing was conducted using LAStools (radpidlasso GmbH, Gilching, Germany, www.rapidlasso.com).

The 30 m DTM was a USGS product derived from Shuttle Radar Topography Mission (SRTM) data (Farr & Kobrick, 2000). To create a 30 m DSM, LANDFIRE Existing Vegetation Height (EVH), a 30 m product, was added to the SRTM-derived

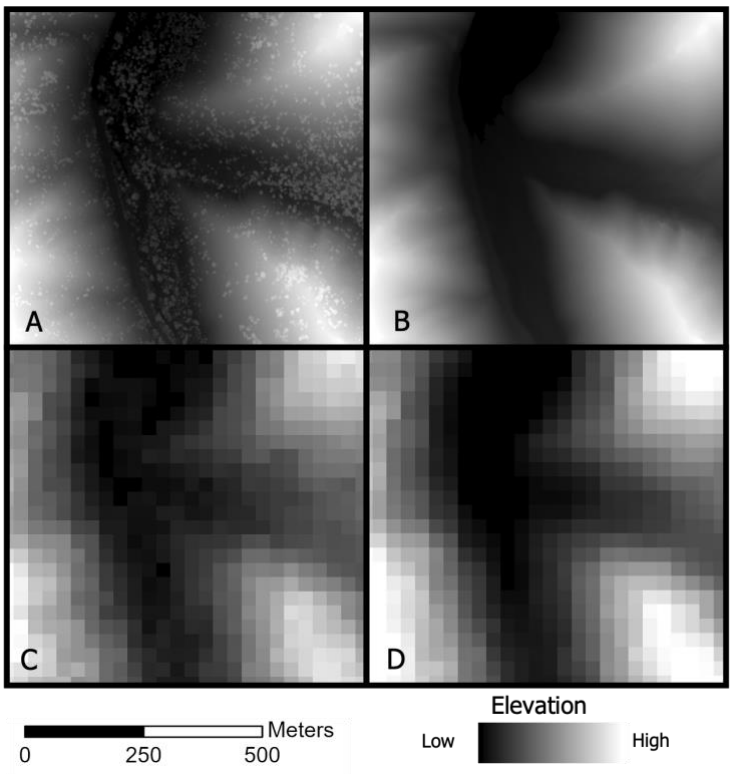

Figure 3. Elevation model comparison. **(A)** 1m DSM , **(B)** 1m DTM, **(C)** 30m DSM, **(D)** 30m DTM.

DEM. EVH reports the average height of the dominant lifeform (e.g. grass, shrub, tree) in each 30 m pixel. Decision-tree models are used to predict heights for EVH, based on field-reference data, lidar, Landsat, and other datasets (LANDFIRE, 2008). For both the 1 m and 30 m DSMs, vegetation height was not reduced within the burn scar of the Green Ridge fire.

3.3 Node Placement

Viewsheds were calculated for each elevation model from the perspective of both crew and fire "nodes". A node represents a single-pixel location of crew or fire perimeter for which a viewshed is calculated. Multiple nodes can be used to represent

the placement of crew on the landscape, or the shape of the fire perimeter. Crew nodes were placed according to features stored in the geospatial incident data acquired from the National Interagency Fire Center (NIFC) for different dates of the Green Ridge fire (Table 1, Figure 4). These features are labeled "completed handlines" which refers to the construction of handlines, a containment tactic that involves crew using handtools to dig or scrape out a fireline (NWCG, 2022). As these handline features are part of the official incident data, they are the most accurate representation available of crew location during fire suppression operations. Crew nodes were placed every 90 m along the handline features, to balance accurately representing crew locations with processing efficiency.

For each handline, complimentary fire nodes were placed on the landscape to represent where the fire was most active for the corresponding date (Figure 4). Infrared imagery, flown over the Green Ridge fire nightly, provides information on fire activity for fire management during suppression. These imagery reports include geospatial features indicating total fire perimeter, intense heat perimeters, and isolated intense heat locations.

Table 1. Summary of nodes placed on landscape for Green Ridge case study. Fire acreage from official Green Ridge incident reports (InciWeb, 2021).

Date	Number of Crew Nodes	Number of Fire Nodes	Fire Growth (acres)	Total Fire (acres)
7/21/21	24	60	1,677	3,245
7/22/21	14	128	666	3,912
7/23/21	7	122	670	4,581
7/25/21	7	108	669	5,883
8/05/21	30	53	1,237	13,488

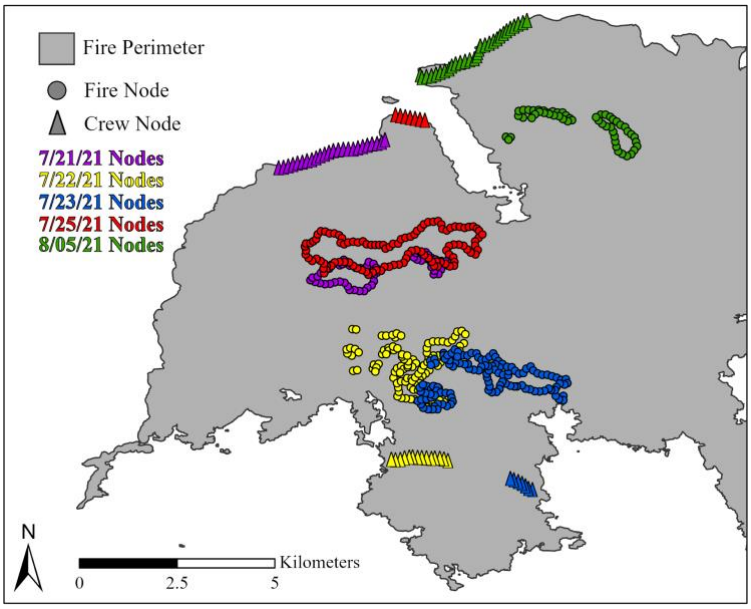

Figure 4. Locations of fire nodes (triangles) and crew nodes (circles), color-coded by date. A Green Ridge fire perimeter from 9/12/21 is shown for reference.

Also available from the NIFC, these official perimeters provide the most accurate record of daily fire progression on the landscape. Intense heat perimeters best represent fire activity per day; as such, fire nodes were placed every 90 m along the perimeter of these polygons for each date corresponding to completed handlines.

3.4 Viewshed Processing

All viewshed processing was done using the ArcPy library in Python 3.7.9. Geodesic Viewshed (also referred to as "Viewshed 2"), released with Esri's ArcGIS Pro 2.7 in 2020, was used to calculate all viewsheds. This algorithm accounts for the curvature of Earth's surface by transforming surface elevations into three-dimensional coordinates and calculating geodesic sightlines (Esri, 2022). Geodesic Viewshed requires an input elevation model and observer point locations; it allows for control

over other elements involved in the calculation such as observer height, and viewshed radius. The resulting viewsheds indicate pixels on the input raster that are visible to one or more observers (Figure 1).

For each date, a total of eight viewsheds were calculated using Geodesic Viewshed: each DEM was considered at both 1 m and 30 m resolution, while both crew and fire nodes were separately considered as observers. Although viewsheds indicate areas on the landscape that can be seen by observers, the inverse is also true. Thus, by mapping viewsheds from a given observer point, you are also mapping areas on the landscape from which the observer point can be seen. In the case of fire and crew nodes, this enables the analysis of landscape-scale crew/node visibility. Viewsheds with crew node inputs had observer elevation explicitly set to that of the terrain, excluding any vegetation, with an offset of 1.7 m to account for average human height. Viewsheds with fire node inputs took their elevation from the input DEM, allowing fire to be simulated on the ground or at the level of vegetation height, depending on the DEM (Figure 5). All viewsheds were restricted to a 3.5 km radius, per node, to balance realistic depth of view with processing time.

Each viewshed calculation resulted in a raster, where each pixel value represented the number of crew or fire nodes from which that pixel was visible. Recalling Figure 1, where there is only one observer, each blue pixel has a viewshed value of 1 which we interpret as 100% of observers can see said blue pixels. Conversely, the blue pixels in Figure 1 could also be interpreted as areas on the landscape that can see 100% of the observers. For the purpose of this study, visibility

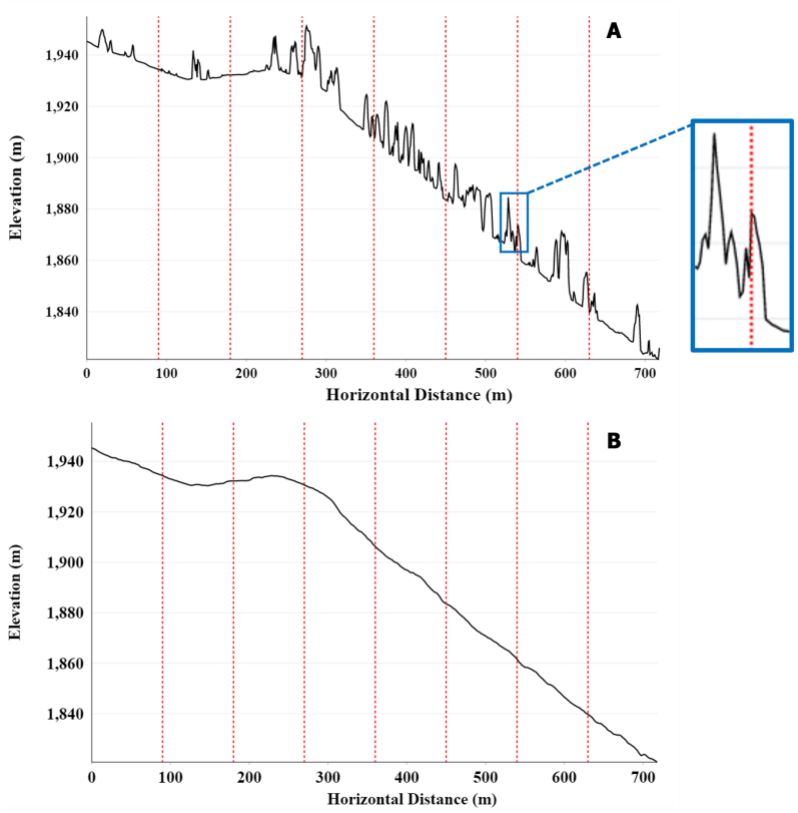

Figure 5. 1m DSM **(A)** and DTM **(B)** profile transects across the 7/23/21 handline shown in Figure 3. Vertical lines indicate node locations. **(A)** shows vegetation presence will influence node location and visibility.

will refer to the percentage of nodes that can see or be seen from a pixel location on the landscape.

Geodesic Viewshed was implemented using graphic processing unit (GPU) processing which allowed for increased performance. A Nvidia Tesla T4 GPU with 320 tensor cores and 16 GB of memory was used for viewshed calculations. 30 m processing times were under one minute, while 1 m processing times varied from 4 hours to > 10 hours, depending on the number of nodes used for processing.

3.4.1 Viewshed Post-Processing

Geodesic Viewshed outputs a raster indicating visible pixels on the landscape, according to input nodes and elevation model. The minimum value is zero, indicating no visibility. The maximum possible value is equal to the number of input crew or fire nodes (Table 1). Owing to the range of the number of input nodes, each viewshed was normalized according to Equation 1:

$$x_{norm} = \frac{x}{\max(x)} \quad (1)$$

where x represents the original visibility value between 0 and the maximum number of input nodes (*max(x)*), x_{norm} is the normalized visibility value, between 0 and 1, where a value of 1 represents a pixel visible by 100% of the input nodes.

In order to understand the distribution of visibility according to input nodes, normalized viewsheds were reclassified according to two thresholds: more than 10% visibility and more than 30% visibility. These reclassified viewsheds represent areas on the landscape that are visible to at least 10% or 30% of nodes, respectively. Recall that original viewsheds represent areas on the landscape that are visible to one or more nodes. These reclassified viewsheds, in addition to the originals, show how visibility is influenced by the number of nodes on the landscape.

Further post-processing was done to determine where crew and fire viewsheds overlap, or areas on the landscape where a lookout would have some degree of visibility of both firefighters and active fire. For each date, according to DEM and resolution, the

crew and fire node viewsheds were summed to obtain all non-zero overlap. Resulting summed visibility has a possible range between 0 and 2. Often, much of this overlapping fire-crew visibility is found between the fire and the crew. However, if this method is to be applied for the identification of possible locations to place a lookout, for whom both crew and fire visibility is important, then the area between fire and crew is unsuitable, given the safety risk. To remove these potentially dangerous areas from consideration, a convex hull between fire and crew nodes was used to exclude the area between a crew and active fire henceforth referred to as the high risk zone (HRZ) (Figure 6C). This approach was applied to overlapping viewsheds to determine the resulting low risk zone (LRZ) (Figure 6D).

3.5 Analysis

Median regression, conducted using the quantreg R package (Koenker 2022, R Core Team 2020), was the main approach used to compare visibility across different models. Median regression was chosen instead of the more traditional ordinary least squares regression because the assumption of normality was not met in the data. Pixel-by-pixel comparisons between DEMs, keeping resolution constant, and between resolutions, using either DTMs or DSMs, were modeled using median regressions (Table 2).

Visibility was plotted on a pixel-by-pixel basis to determine the degree of agreement across DEMs and resolution by fitting a median regression model. For comparisons across DEMs (holding resolution constant), the slope of the median regression describes how much visibility is lost with the addition of vegetation on the

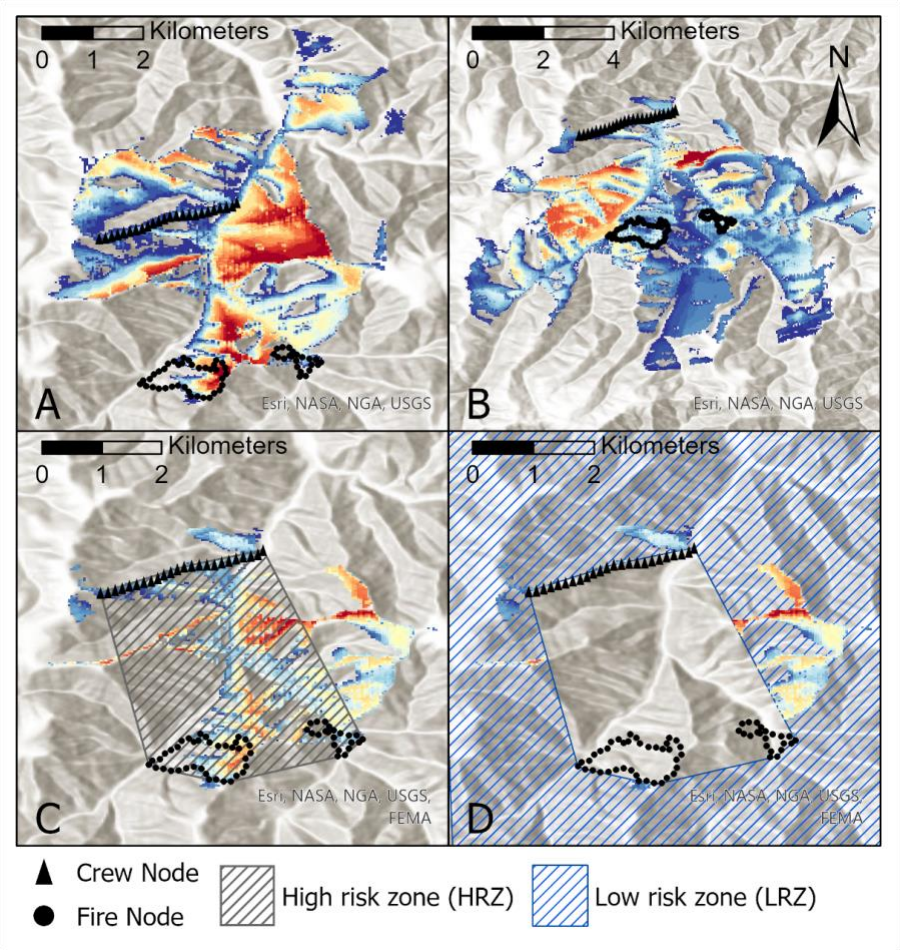

Figure 6. Example viewsheds for 30 m DTM on 7/21/21 [lowest visibility (blue), highest visibility (red)]. **(A)** Crew node visibility [0.04, 0.92] **(B)** Fire node visibility [0.02, 0.8] **(C)** Overlapping visibility, HRZ and LRZ [0.06, 1.51] **(D)** LRZ visibility, HRZ excluded based on a convex hull around crew and fire nodes [0.06, 1.51].

Table 2. Summary of pixel-by-pixel comparisons modeled using quantile regression.

Comparison Type	Constant	Node Type
DEM	30 m resolution	Crew
DEM	30 m resolution	Fire
Resolution	DTM	Crew
Resolution	DTM	Fire
Resolution	DSM	Crew
Resolution	DSM	Fire

landscape. Complementarily, comparing across resolutions, the slope describes the prevailing trends in differences between fine and coarse resolution data.

In order to accomplish a pixel-by-pixel analysis across resolutions, all 1 m viewsheds were aggregated to 30 m using mean aggregation. The mean aggregation takes the average value of all 1m pixels, in a $30m^2$ area, and applies that average as the new 30 m pixel value. The output is a new raster representative of 1m visibility at a 30m resolution. Since resolution comparisons consistently use either the DTM or DSM, indirect comparisons could be made regarding the influence of resolution across DEMs, including for highly visible, safer LRZ locations.

CHAPTER 4

RESULTS

4.1 Visibility

Overall, visibility in the high-elevation, forested landscape of the Green Ridge fire in southeastern Washington was limited (Table 3). On average, the 30 m DTM, using fire nodes as observers, resulted in the largest visible percentage of the landscape (36.46%). However, our most realistic model (1m DSM) resulted in the two lowest average visible percentages of the landscape at just 8.32% for crew nodes and 11.38% for fire nodes (Table 3). All 30 m models, regardless of DEM, overestimated visible area by as little as 6% or as much as 24%, when compared with their 1m counterparts. DTMs also significantly overestimated visible area compared with DSMs, by as much as 14%. However, the overestimation by DTMs was more significant for crew nodes than fire nodes. Further, crew nodes generally saw smaller percentages of the landscape compared with fire nodes.

When introducing thresholds for visibility, the visible area decreased across all model types regardless of node type, resolution, or DEM (Table 3, Figure 7). A 10% threshold severely restricted visible areas, but all model types retained some degree of visibility across the landscape. The same was not true using a 30% threshold, where several model combinations forfeited any visible area (Table 3). When restricting

Table 3. Percentages of the landscape visible to crew and fire nodes for each date, elevation model, and resolution. All nodes, more than 30% of nodes, and more than 10% of nodes are considered as thresholds for visibility.

Date	DEM	Resolution (m)	Percent visible to…					
			at least 1 crew node	at least 1 fire node	more than 10% of crew nodes	more than 10% of fire nodes	more than 30% of crew nodes	more than 30% of fire nodes
7/21	DTM	30	22.59	40.63	19.28	26.57	13.71	8.07
		1	18.48	16.47	15.20	13.77	9.62	2.25
	DSM	30	21.27	39.19	17.95	25.62	11.78	7.84
		1	9.36	12.21	5.85	1.63	1.47	0
7/22	DTM	30	21.06	31.28	17.98	16.03	12.36	4.35
		1	13.44	25.47	12.18	9.20	7.93	0.69
	DSM	30	11.28	31.18	16.16	15.31	10.22	3.90
		1	1.53	7.12	0.81	0.01	0	0
7/23	DTM	30	15.31	33.54	15.30	12.57	0	3.63
		1	8.80	26.71	8.79	8.03	0	1.02
	DSM	30	9.83	32.66	9.83	11.59	0	3.44
		1	0.14	7.73	0.15	0.13	0	0
7/25	DTM	30	23.31	42.08	23.32	22.95	15.99	4.38
		1	15.63	33.12	15.63	12.04	11.23	0.95
	DSM	30	16.72	41.13	16.70	22.08	10.58	4.10
		1	15.63	16.08	8.12	1.65	4.40	0
8/5	DTM	30	35.14	34.77	25.17	21.29	15.74	6.94
		1	29.47	27.74	18.76	11.92	10.77	2.05
	DSM	30	30.46	33.75	20.81	20.38	12.19	6.58
		1	14.95	13.76	7.07	2.08	2.15	0.05
All dates average	DTM	30	23.49	36.46	20.21	19.88	11.56	4.79
		1	17.17	25.90	14.11	10.99	7.91	2.08
	DSM	30	17.91	35.58	16.29	18.99	8.95	4.35
		1	8.32	11.38	4.40	1.10	1.60	0.83

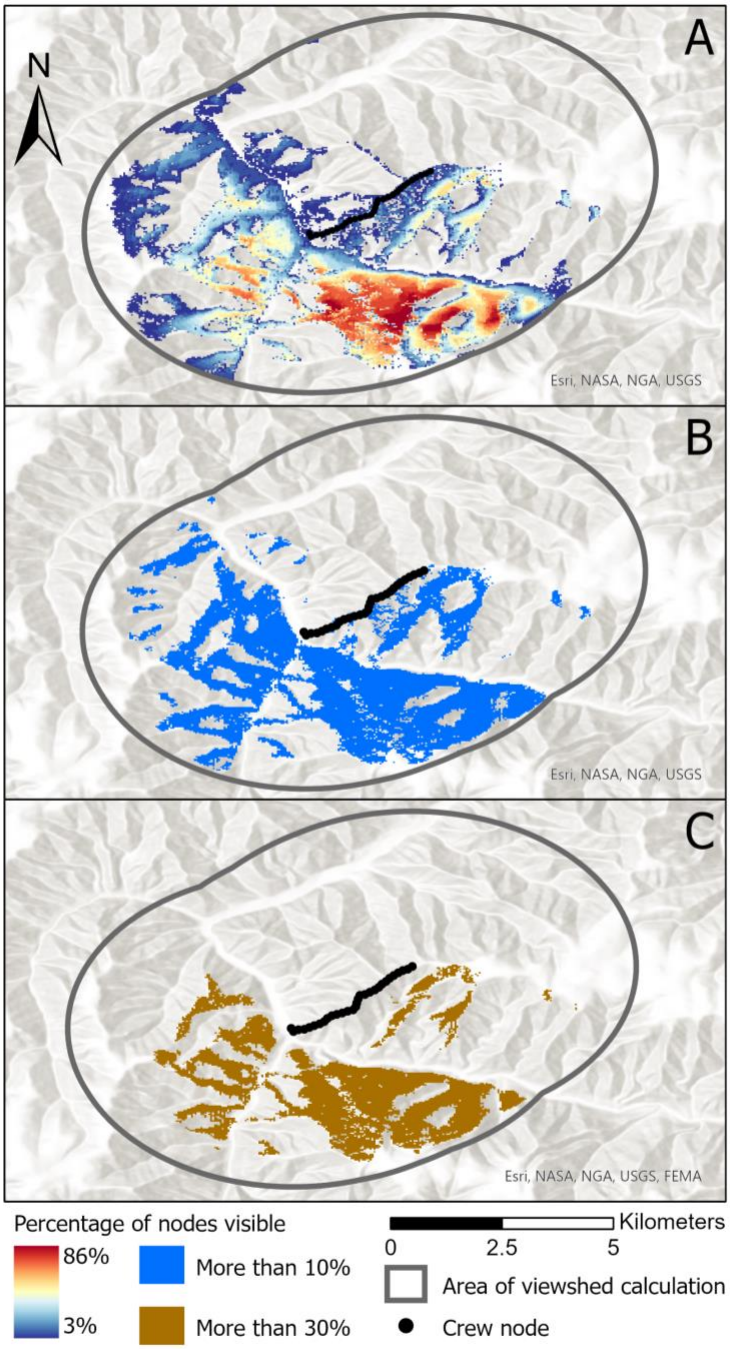

Figure 7. Example viewsheds for crew nodes, 30 m DSMs on 8/05/21. **(A)** Visibility of one or more nodes. **(B)** Visibility of more than 10% of nodes. **(C)** Visibility of more than 30% of nodes.

viewsheds by any threshold, fire nodes' visible area, on average, was more affected than that of crew nodes. For example, when imposing a 10% threshold, the difference in percentage visible area for crew nodes decreased by an average of 3% (across all model types). For fire nodes, this difference in percentage visible was 15%. When imposing a 30% threshold, crew nodes again maintained a higher average percentage visible area, with a difference of just 9% versus 24% for fire nodes.

4.2 Median Regression

Six median regressions capture the differences across resolutions and DEM types, accounting for different node types. Three categories per node type are considered: a DEM comparison between 30 m viewsheds, a resolution comparison for DTM-based viewsheds, and a resolution comparison for DSM-based viewsheds (Figure 8, Figure 9). The explanatory variable for each regression is that of the model which added more complexity to the landscape (whether that be 1 m resolution, or a DSM), and therefore the slope of the regression provides a measure of how well visibility is explained when adding more detail to the landscape on which visibility is calculated. The DEM comparison (DTM versus DSM at 30m) provided the highest slopes, 0.98 and 0.71 for fire and crew nodes, respectively (Figure 8). For fire nodes at 30 m, the addition of vegetation height (DSM visibility) results in 98% of the visibility produced without vegetation (DTM visibility). However, for crew nodes, only 71% of visibility is captured using a 30m DSM as compared to a DTM.

Resolution comparison regressions resulted in lower slopes, but also saw DTM-based comparisons with higher slopes than DSM-based models (Figure 9). Contrary to

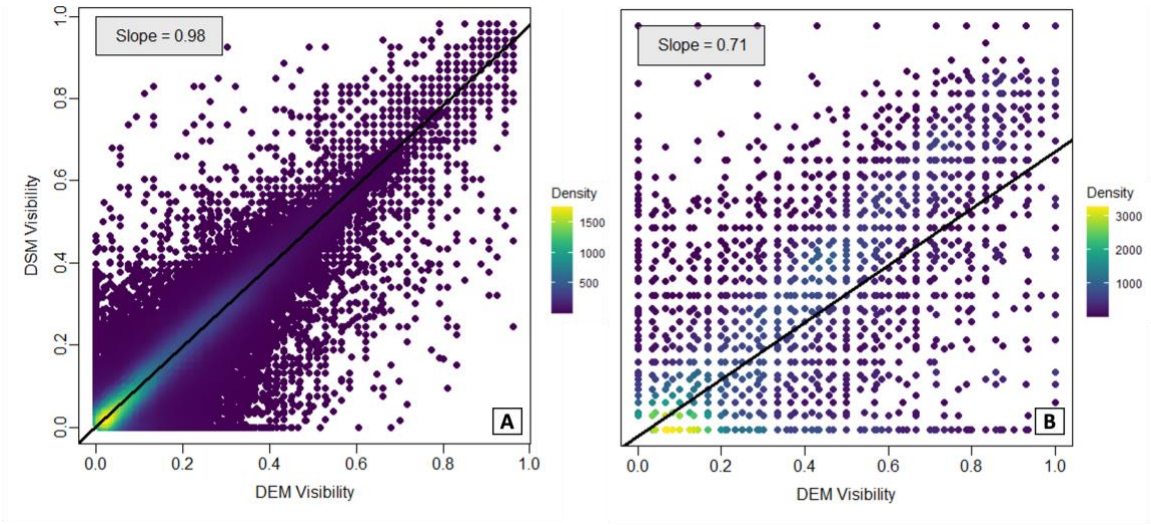

Figure 8 Regressions for 30 m elevation model comparisons. A: Fire nodes B: Crew nodes. Density refers to point density, or the number of points plotted at the same (x,y) location.

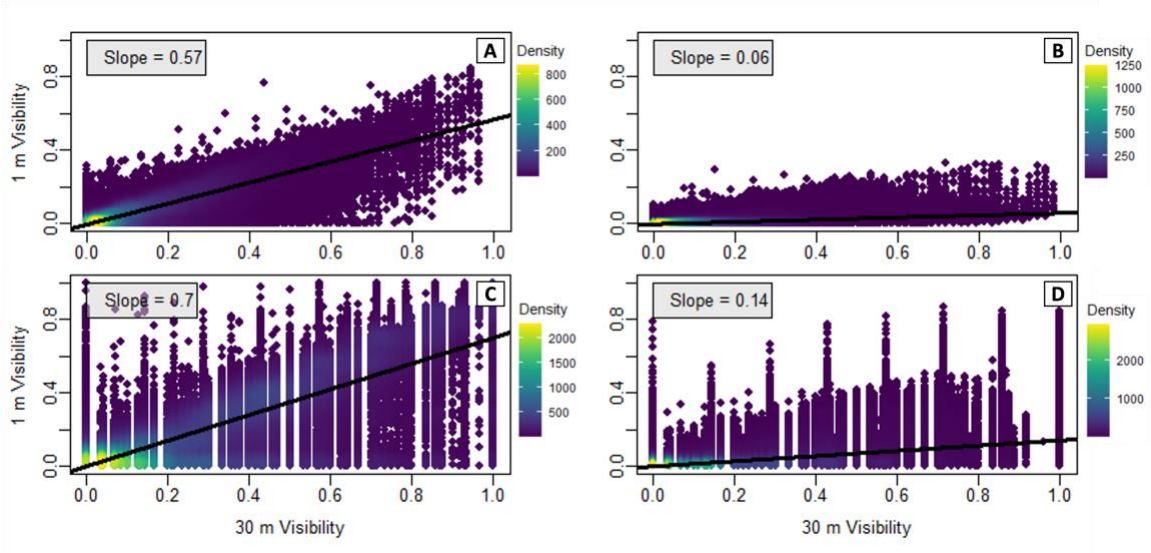

Figure 9. Regressions for resolution comparisons. A: Fire nodes, DTM B: Fire nodes, DSM C: Crew nodes, DTM D: Crew nodes, DSM. Density refers to point density, or the number of points plotted at the same (x,y) location.

the DEM comparison plots, crew nodes generally produced higher slopes than fire nodes, for their respective DEM. The detail provided by a DSM at 1m predicts just 6% of the visibility at 30m for fire nodes and 14% for crew nodes. Excluding vegetation detail at higher resolution still only predicts 57% of the visibility for fire nodes and 70% for crew nodes. Regardless of DEM or resolution, each plot demonstrates how much more widespread areas of low visibility are compared to areas of high visibility owing to the significant point density concentration at low visibility values (Figure 8, Figure 9).

4.3 Visible Area and Overlap

Visible area is highly dependent on node type, DEM type, and resolution (Table 4, Figure 6). Crew visible area is generally higher when modeled at 30m, across both DEMs; however DTMs generally model more area than DSMs for both node type as well. Fire visible area is generally higher at 30m, across DEMs, with DTMs only slightly outperforming DSMs, compared with crew nodes.

Overlapping crew and fire viewsheds present significantly limited visible areas at both resolutions, with most visible areas occurring between the fire and crew nodes. All overlapping viewsheds have more visible area from 30m models than 1m. LRZs were even further spatially limited, by excluding potentially dangerous terrain directly between crew and fire nodes. Following the trend of general visibility, DSM LRZs were significantly smaller than those of the DEMs. Resolution also played a big factor here, with 30 m consistently overestimating the area of an LRZ (Table 4). On average, DSMs have a greater difference between overlap area modeled at 30 m versus 1m, with 30 m DSMs over-predicting overlap by an average of 2.6 km^2. DEMs were not far behind with

Table 4. Visible area in km^2 describing overlapping visibility. Percent safe refers to the LRZ in km^2 modeled at 1m over the LRZ in km^2 modeled at 30m, multiplied by 100.

Date	DEM	Resolution	Crew Visible Area	Fire Visible Area	Overlap Visible Area	LRZ Visible Area	Percent Safe
7/21	DTM	30	11.93	24.08	4.69	1.43	58.74
		1	9.76	18.3	2.67	0.84	
	DSM	30	11.23	23.23	4.3	1.34	21.64
		1	4.94	7.24	0.7	0.29	
7/22	DTM	30	9.62	20.65	4.42	2.5	45.6
		1	6.14	16.81	2.4	1.14	
	DSM	30	5.15	20.58	1.33	0.73	1.37
		1	0.7	4.7	0.01	0.01	
7/23	DTM	30	6.42	22.03	1.63	0.47	57.45
		1	3.69	17.54	1.09	0.27	
	DSM	30	4.12	21.45	0.72	0.28	0.36
		1	0.06	5.08	0.001	0.001	
7/25	DTM	30	9.86	28.73	2.39	1.82	52.2
		1	6.61	22.61	1.17	0.95	
	DSM	30	7.07	28.08	2	1.68	21.43
		1	6.61	10.98	0.42	0.36	
8/05	DTM	30	19.58	21.05	8.35	4.54	65.86
		1	16.42	16.79	5.55	2.99	
	DSM	30	16.97	20.43	7.51	4.18	24.64
		1	7.12	8.33	1.58	1.03	

30 m models over-predicting overlap by an average of 1.7 km^2. These values are significant considering the overlap area for each of these categories is quite small (Table 4).

LRZs followed the same pattern, with 30 m DSMs and DTMs over-predicting by 1.3km^2 and 30m DEMs over-predicting by 0.91 km^2 , for even smaller areas. The percentage of LRZ areas modeled at 1m compared to 30 m (Table 4) is always less than 100, confirming that 30m models are consistently overestimating LRZs. For one date, 7/23/21, just 0.36% of the 30 m LRZ is also deemed a 1 m LRZ according to the DSM

model. These percentages are significantly higher for DEM models, with an average of 55.97%, compared to DSM models, with an average of just 13.89%.

CHAPTER 5

DISCUSSION

The results of this research can be interpreted through two distinct lenses: that of a GIS user, and that of a fire professional. The implications for a GIS user stem from the results of comparing model resolution and model type, as these are frequently investigated concerns (Fisher et al., 2018; Vukomanovic et al., 2018). A decision-maker, such as a member of an incident command team or wildland firefighter, is likely more concerned with practical implications of the research: what can these results tell us about improving safety on the job?

Overall low visibility is expected in a forested, mountainous landscape. In general, crew nodes can see a smaller percentage of the landscape than fire nodes (keeping resolution and model type constant). However, a notable influence on these results is the ability of fire nodes to "see" from treetops (observer elevation taken from the landscape) versus crew nodes which are forced to take their vantage point from the elevation/height of a typical human observer (1.7 m above the bare-earth elevation). Additionally, for each date, there are anywhere from 1.7 to 17 times as many fire nodes as crew nodes, providing greater diversity in elevation and aspect. However this difference is mitigated when analyzing the percentage of a landscape that is visible, a calculation which accounts for the larger area covered by more nodes.

Another notable difference between crew and fire nodes is that crew nodes maintain larger portions of visible areas despite the imposition of a threshold of 10% or 30% on the original viewshed. This suggests that crew nodes may be better positioned overall to see a landscape, perhaps owing to the likelihood that a handline is constructed somewhere with naturally better visibility (e.g., near a ridgeline to reinforce a natural fire break). It may also suggest that fire nodes' ability to see larger areas is dependent on a few well-positioned nodes, which, when removed, severely restrict visible areas.

5.1 GIS Implications

5.1.1 Elevation Model Comparison

Owing to their inclusion of vegetation as an opaque barrier on the landscape, DSMs are inherently more restrictive in their ability to model visibility. However, this restriction also paints a more realistic picture of the landscape, especially in a forested environment where a DEM severely oversimplifies the landscape. The slopes of our median regressions between 30m DEM modeled visibility and 30 m DSM modeled visibility (Figure 6), support that a DSM is more restrictive in its modeling of visibility.

However, at 30m for fire nodes, a DSM captures 98% of the visibility captured by a DTM model. However, for crew nodes, a DSM only captures 71% of the visibility produced by a DTM model of the same resolution. The lower slope for crew nodes is likely a result of the observer elevation setting mentioned in the previous section, where visibility from the surface is much more restricted, while visibility from the top of the DSM landscape is only slightly more restricted than when using a DTM (Figure 5).

These results further confirm that DTMs oversimplify a landscape and modeling

visibility using DTMs will overestimate visibility (Murgoitio et al., 2013; Vukomanovic et al., 2018). However, it is important to note that while a DSM may provide more detail to the landscape by including vegetation, all vegetation is assumed to be opaque, which is a more restrictive oversimplification of reality (Doneus et al., 2022; Bartie et al., 2011; Murgoitio et al., 2013). Therefore, we must balance our interpretation to account for the fact that the DSM estimation of visibility may be overly restrictive.

5.1.2 Resolution Comparison

Similar to a DSM providing more realistic surface representation than a DTM, finer resolution should also more realistically model topography. Therefore, our most realistic model is that of the 1m DSM-based. The slopes comparing resolution (Figure 8) suggest that regardless of DEM type or node type, visibility using 30 m models overestimate visibility. DTM-based resolution comparisons also show higher slopes than that of DSM-based resolution comparisons, further suggesting the overestimation of less-realistic models (DEM, 30m). Further, the most realistic model produces the smallest slopes, suggesting that true visibility is most severely overestimated by these models.

These results confirm that modeling visibility using coarse resolution significantly overestimates visibility. However, it is possible that our most realistic model is too restrictive due to EM type and resolution. While 1m data provides a more realistic landscape, it also restricts observers to $1m^2$ areas, versus $900m^2$ areas at coarse resolution. Realistically a crew member may traverse $>1m^2$ to assess surrounding visibility. This may contribute to a slight underestimation of visibility by the 1m models, especially those using DSMs. While the 1m DSM may provide the most realistic model,

it may not be the most realistic method for analysis owing to limited data availability, high volume required for data storage, and lengthy processing times of up to 10 hours per viewshed.

5.2 Wildland Firefighter Implications

Generally, low visibility is not a surprising result when considering most wildfires occur in forested areas with rugged terrain that naturally limits visibility. However, the ability to model such visibility may be useful in planning mitigation efforts. Knowing our models overestimate visibility at course resolutions/using DTMs, these models may provide a false sense of security when entering these areas for wildland firefighting efforts.

Areas where a wildland firefighter could potentially see both their crew and nearby fire hazard are relatively rare in mountainous, forested landscapes. When present, these areas are quite small and significantly overestimated by the simpler models. However, methods do exist to successfully map these areas with room to improve accuracy. With improvement, there is potential to use these methods to map highly visible areas of an active fire, to increase situational awareness. Differences between DTMs and DSMs may be less of an issue for maintaining communications, since vegetation will provide less of an impediment to radio communications than to visible line-of-sight.

Future work should address realistic modeling of crew and fire location, specifically accounting for crew movement beyond $1m^2$ areas. Further, accounting for fire behaviors such as crown fire versus surface when placing fire nodes may further

increase our ability to accurately model visibility. However, these methods are intended for increasing situational awareness in the planning stage rather than in real-time response to mitigation efforts and fire behavior.

While avenues exist to improve these modeling efforts, the processing power and time required for the best models is a major consideration for implementing these visibility models. Modeling 1m viewsheds from 30m data should be considered as a way to bridge this major processing requirement.

This study does not consider other impacts on visibility found in wildland fire landscapes. One major influence on visibility surrounding an active fire is smoke. Not only the presence of smoke but the combination of intense fire behavior, with severe weather such as high winds, may produce varied impacts on visibility that are not accounted for in these models. Not only will fire behavior alter smoke effects, it will also determine flame height/shape which alters visibility in a different way. For example, a crown fire with 10 m flames is much more visible than that of flames on the surface.

Another dynamic aspect of a wildland fire environment is the removal of fuel, both through burning and mitigation efforts. Our models do not account for burned vegetation altering the visibility as captured by pre-fire lidar. Depending on the severity of the fire, burned vegetation may be reduced significantly in height, or have more through-vegetation visibility owing to fewer leaves/branches present. Mitigation efforts such as bulldozing lines and digging handlines may also alter the landscape in a way that changes visibility. These landscape changes are not accounted for in this study's modeling. Another limitation of this study is the conversion of lidar point clouds into pixel-based rasters. Using a raw point cloud to calculate visibility (Lecigne et al., 2020),

rather than even a very fine-scale raster, may provide compelling results, especially in areas where vegetation is widespread.

Despite the limitations, this research may be successfully incorporated with existing research to improve firefighter safety outcomes. For example, safety zone mapping relies on existing vegetation type and elevation to determine areas of sufficient safety for wildland fires (Campbell et al., 2022). Visibility analysis could easily be incorporated into these calculations to provide further information about the safety zones. For example, a safety zone may meet all requirements to shelter a crew, but if it has severely restricted visibility it may be a less desirable place to send a crew. Additionally, the Escape Route Index (ERI) developed by Campbell et al., 2019 could incorporate visibility analyses to further characterize the safety of these routes in an active fire situation. Overall this work could contribute to wildland fire mitigation efforts by presenting further metrics for determining the safety of areas wildland firefighters may be sent to work.

CHAPTER 6

CONCLUSION

This study compared methods for mapping fire and firefighter visibility in order to improve situational awareness. The results showed that visibility is overestimated when modeled using simplified landscape models and coarse resolution. An omission of vegetation from the landscape overestimates visibility by up to 29% at the 30m level. However, even when using a more detailed DSM model, using coarse resolution topography models overestimates visibility by 94% for fire nodes and 86% for crew nodes. The most realistic model, using a 1m DSM, produced the most limited visible areas in terms of both average visibility and total visible area.

Further, overlapping visibility is severely limited at the 1m DSM level, suggesting a lack of areas that realistically provide good visibility of both wildland firefighter crew and active fire hazard. However, mapping these areas could significantly improve situational awareness by allowing incident managers to assess visibility of planned handline locations, safety zones, or escape routes.

Certain improvements are necessary to bring visibility modeling into practical application. Most importantly, hardware and significant processing time for 1m data is prohibitive. Future work should address this by attempting to model fine-scale visibility focusing on realistic processing times and data storage requirements. Further refinements

should focus on addressing assumptions that over- or under-estimate visibility, such as opaque vegetation and an observer's ability to move on the landscape.

REFERENCES

Abatzoglou, J. T., Battisti, D. S., Williams, A. P., Hansen, W. D., Harvey, B. J., & Kolden, C. A. (2021). Projected increases in western US forest fire despite growing fuel constraints. *Communications Earth & Environment 2*(1), 227. https://doi.org/10.1038/s43247-021-00299-0

Alexander, M. E., & Cruz, M. G. (2006). Evaluating a model for predicting active crown fire rate of spread using wildfire observations. *Canadian Journal of Forest Research*, *36*(11), 3015–3028. https://doi.org/10.1139/X06-174

Allison, R. S., Johnston, J. M., Craig, G., & Jennings, S. (2016). Airborne optical and thermal remote sensing for wildfire detection and monitoring. *Sensors (Switzerland)*, *16*(8), 1310. https://doi.org/10.3390/s16081310

Arizona State Forestry Division. (2013). Yarnell Hill Fire: Serious Accident Investigation Report. https://wildfiretoday.com/documents/Yarnell_Hill_Fire_report.pdf (accessed on 18 March 2022).

Baek, H. & Lim, J., (2018) Design of future UAV-relay tactical data link for reliable UAV control and situational awareness. *IEEE Communications Magazine*, 56(10), 144-150, https://doi.org/10.1109/MCOM.2018.1700259

Balch, J. K., Schoennagel, T., Williams, A. P., Abatzoglou, J. T., Cattau, M. E., Mietkiewicz, N. P., & Denis, L. A. S. (2018). Switching on the big burn of 2017. *Fire*, *1*(1), 1–9. https://doi.org/10.3390/fire1010017

Barmpoutis, P., Papaioannou, P., Dimitropoulos, K., & Grammalidis, N. (2020). A review on early forest fire detection systems using optical remote sensing. *Sensors (Switzerland)*, *20*(22), 1–26. https://doi.org/10.3390/s20226442

Bartie, P., Reitsma, F., Kingham, S., & Mills, S. (2011). Incorporating vegetation into visual exposure modelling in urban environments. *International Journal of Geographical Information Science*, *25*(5), 851–868. https://doi.org/10.1080/13658816.2010.512273

Beighley, M. (1995). Beyond the safety zone: Creating a margin of safety. *Fire Management Notes*, 55(5), 22–24.

Campbell, M. J., Dennison, P. E., & Butler, B. W. (2017). A LiDAR-based analysis of the effects of slope, vegetation density, and ground surface roughness on travel rates for wildland firefighter escape route mapping. *International Journal of Wildland Fire*, *26*(10), 884–895. https://doi.org/10.1071/WF17031

Campbell, M. J., Dennison, P. E., Thompson, M. P., & Butler, B. W. (2022). Assessing potential safety zone suitability using a new online mapping tool. *Fire*, *5*(1), 5. https://doi.org/10.3390/fire5010005

Campbell, M. J., Dennison, P. E., & Butler, B. W. (2017). Safe separation distance score: A new metric for evaluating wildland firefighter safety zones using lidar. *International Journal of Geographical Information Science*, *31*(7), 1448–1466. https://doi.org/10.1080/13658816.2016.1270453

Campbell, M. J., Dennison, P. E., Butler, B. W., & Page, W. G. (2019). Using crowdsourced fitness tracker data to model the relationship between slope and travel rates. *Applied Geography*, *106*(March), 93–107. https://doi.org/10.1016/j.apgeog.2019.03.008

Campbell, M. J., Page, W. G., Dennison, P. E., & Butler, B. W. (2019). Escape route index: A spatially-explicit measure of wildland firefighter egress capacity. *Fire*, *2*(3), 1–19. https://doi.org/10.3390/fire2030040

Chamberlain, B. C., & Meitner, M. J. (2013). A route-based visibility analysis for landscape management. *Landscape and Urban Planning*, *111*(1), 13–24. https://doi.org/10.1016/j.landurbplan.2012.12.004

Dean, D. J. (1997) Improving the accuracy of forest viewsheds using triangulated networks and the visual permeability method. *Canadian Journal of Forest Research*, 27(7), 969–977. https://doi.org/10.1139/x97-062

Dennison, P. E., Fryer, G. K., & Cova, T. J. (2014b). Identification of firefighter safety zones using lidar. *Environmental Modelling and Software*, *59*, 91–97. https://doi.org/10.1016/j.envsoft.2014.05.017

Dennison, P. E., S. C. Brewer, J. D. Arnold, & M. A. Moritz (2014a). Large wildfire trends in the western United States, 1984–2011, *Geophysical Research Letters*, *41*(8), 2928–2933, https://doi.org/10.1002/2014GL059576

Doneus, M., Banaszek, Ł., & Verhoeven, G. J. (2022). The impact of vegetation on the visibility of archaeological features in airborne laser scanning datasets from different acquisition dates. *Remote Sensing*, *14*(4), 858. https://doi.org/10.3390/rs14040858

Egan, T. (2009). *The big burn: Teddy Roosevelt and the fire that saved America.* Houghton Mifflin Harcourt.

ESRI. (2022). How Geodesic Viewshed works. ArcGIS Pro. https://pro.arcgis.com/en/pro-app/2.8/tool-reference/spatial-analyst/how-viewshed-2-works.htm

Farr, T. G., & Kobrick, M. (2000), Shuttle radar topography mission produces a wealth of data. *Eos, Transactions American Geophysical Union, 81*(48), 583–583. https://doi.org/10.1029/EO081i048p00583

Fisher, P., Farrelly, C., Maddocks, A., & Ruggles, C. (1997). Spatial analysis of visible areas from the Bronze Age cairns of Mull. *Journal of Archaeological Science*, *24*(7), 581–592. https://doi.org/10.1006/jasc.1996.0142

Fisher, J. R. B., Acosta, E. A., Dennedy-Frank, P. J., Kroeger, T., & Boucher, T. M. (2018). Impact of satellite imagery spatial resolution on land use classification accuracy and modeled water quality. *Remote Sensing in Ecology and Conservation*, *4*(2), 137–149. https://doi.org/10.1002/rse2.61

Gargoum, S. A., & Karsten, L. (2021). Virtual assessment of sight distance limitations using LiDAR technology: Automated obstruction detection and classification. *Automation in Construction*, *125*(February), 103579. https://doi.org/10.1016/j.autcon.2021.103579

Gillespie, B. M., Gwinner, K., Fairweather, N., & Chaboyer, W. (2013). Building shared situational awareness in surgery through distributed dialog. *Journal of Multidisciplinary Healthcare*, *6*, 109–118. https://doi.org/10.2147/JMDH.S40710

Gleason, P. (1991). *Lookouts, communication, escape routes and safety zones*. Wildland Fire Leadership Development. https://www.nwcg.gov/sites/default/files/wfldp/docs/lces-gleason.pdf

Graafland, M., Schraagen, J. M. C., Boermeester, M. A., Bemelman, W. A., & Schijven, M. P. (2015). Training situational awareness to reduce surgical errors in the operating room. *British Journal of Surgery*, *102*(1), 16–23. https://doi.org/10.1002/bjs.9643

Grosvenor, J. R. (1999). *A history of the architecture of the USDA Forest Service.* United States Department of Agriculture, Forest Service. https://foresthistory.org/wp-content/uploads/2020/01/History-of-Architecture-in-USFS.pdf

InciWeb. (2021, October 21). Green Ridge Fire Information - InciWeb the Incident Information System. https://inciweb.nwcg.gov/incident/7628/

Kinaneva, D., Hristov, G., Raychev, J., & Zahariev, P. (2019). Early forest fire detection using drones and artificial intelligence. In *2019 42nd International Convention on Information and Communication Technology, Electronics and Microelectronics (MIPRO)* (pp. 1060-1065). IEEE. https://doi.org/10.23919/MIPRO.2019.8756696

Koenker, R. (2022). quantreg: Quantile Regression. R package version 5.88. [Software] https://CRAN.R-project.org/package=quantreg

Lahaye, S., Sharples, J., Matthews, S., Heemstra, S., Price, O., & Badlan, R. (2018). How do weather and terrain contribute to firefighter entrapments in Australia? *International Journal of Wildland Fire*, *27*(2), 85–98. https://doi.org/10.1071/WF17114

LANDFIRE. (2008) Existing vegetation type, U.S. Department of the Interior, Geological Survey, and U.S. Department of Agriculture. [Image file]. http://landfire.cr.usgs.gov/viewer/.

LAStools. Efficient LiDAR Processing Software. [Software]. http://rapidlasso.com/LAStools

Lecigne, B., Eitel, J. U. H., & Rachlow, J. L. (2020). viewshed3d: An r package for quantifying 3D visibility using terrestrial lidar data. *Methods in Ecology and Evolution*, *11*(6), 733–738. https://doi.org/https://doi.org/10.1111/2041-210X.13385

Lefsky, M. A., Cohen, W. B., Parker, G. G., & Harding, D. J. (2002). Lidar remote sensing for ecosystem studies. *BioScience*, *52*(1), 19–30. https://doi.org/10.1641/0006-3568(2002)052[0019:LRSFES]2.0.CO;2

Llobera, M. (2007). Modeling visibility through vegetation. *International Journal of Geographical Information Science*, *21*(7), 799–810. https://doi.org/10.1080/13658810601169865

Mangan, R. J. (2001). *Investigating wildland fire entrapments*. United States Department of Agriculture, Forest Service, Technology & Development Program. https://www.fs.fed.us/eng/pubs/pdfpubs/pdf95512845.pdf

Matt Jolly, W., & Freeborn, P. H. (2017). Towards improving wildland firefighter situational awareness through daily fire behaviour risk assessments in the US Northern Rockies and Northern Great Basin. *International Journal of Wildland Fire*, *26*(7), 574–586. https://doi.org/10.1071/WF16153

Murgoitio, J. J., Shrestha, R., Glenn, N. F., & Spaete, L. P. (2013). Improved visibility calculations with tree trunk obstruction modeling from aerial LiDAR. *International Journal of Geographical Information Science, 27*(10), 1865–1883. https://doi.org/10.1080/13658816.2013.767460

National Interagency Fire Center. (2021). 2021 incidents, Washington: Green Ridge. [Geodatabase] https://ftp.wildfire.gov/public/incident_specific_data/pacific_nw/Z_2021_HISTORIC/2021_Incidents_Washington/2021_GreenRidge_OR-UMF_000659/

National Park Service. (2021) Wildland Fire in Lodgepole Pine. https://www.nps.gov/articles/wildland-fire-lodgepole-pine.htm

National Wildfire Coordinating Group. (2017). NWCG report on wildland firefighter fatalities in the United States: 2007-2016. https://www.nwcg.gov/sites/default/files/publications/pms841.pdf

National Wildfire Coordinating Group (2022) Glossary A-Z. https://www.nwcg.gov/glossary/a-z

Nofi, A. A. (2000). *Defining and measuring shared situational awareness*. Center For Naval Analyses, Alexandria VA. https://www.cna.org/cna_files/pdf/ D0002895.A1.pdf

Page, W. G., & Butler, B. W. (2018). Fuel and topographic influences on wildland firefighter burnover fatalities in Southern California. *International Journal of Wildland Fire*, *27*(3), 141–154. https://doi.org/10.1071/WF17147

Page, W. G., Freeborn, P. H., Butler, B. W., & Jolly, W. M. (2019). A classification of US wildland firefighter entrapments based on coincident fuels, weather, and topography. *Fire*, *2*(4), 1–23. https://doi.org/10.3390/fire2040052

Page, W. G., Freeborn, P. H., Butler, B. W., & Jolly, W. M. (2019). A review of US wildland firefighter entrapments: Trends, important environmental factors and research needs. *International Journal of Wildland Fire*, *28*(8), 551–569. https://doi.org/10.1071/WF19022

Pastor, E., Zárate, L., Planas, E., & Arnaldos, J. (2003). Mathematical models and calculation systems for the study of wildland fire behaviour. *Progress in Energy and Combustion Science*, *29*(2), 139–153. https://doi.org/10.1016/S0360-1285(03)00017-0

R Core Team (2020). R: A language and environment for statistical computing. R Foundation for Statistical Computing, https://www.R-project.org/.

Salis, M., Arca, B., Alcasena, F., Arianoutsou, M., Bacciu, V., Duce, P., Duguy, B., Koutsias, N., Mallinis, G., Mitsopoulos, I., Moreno, J. M., Pérez, J. R., Urbieta, I. R., Xystrakis, F., Zavala, G., & Spano, D. (2016). Predicting wildfire spread and behaviour in Mediterranean landscapes. *International Journal of Wildland Fire*, *25*(10), 1015–1032. https://doi.org/10.1071/WF15081

Schroeder, W., Oliva, P., Giglio, L., & Csiszar, I. A. (2014). The New VIIRS 375m active fire detection data product: Algorithm description and initial assessment. *Remote Sensing of Environment*, *143*, 85–96. https://doi.org/10.1016/j.rse.2013.12.008

Stanton, N. A., Chambers, P.R., & Piggott, J. (2001). Situational awareness and safety *Safety Science, 39*(3), 189–204. https://doi.org/10.1016/S0925-7535(01)00010-8

Sullivan, P. R., Campbell, M. J., Dennison, P. E., Brewer, S. C., & Butler, B. W. (2020). Modeling wildland firefighter travel rates by terrain slope: Results from GPS-tracking of type 1 crew movement. *Fire*, *3*(3), 1–14. https://doi.org/10.3390/fire3030052

U.S. Geological Survey, 20190515, USGS Lidar Point Cloud WA 3 County QL1 2017 WA3 LAS. (2019). U.S. Geological Survey. https://nationalmap.gov/3DEP/

U.S. Geological Survey, 20190513, USGS Lidar Point Cloud WA 3 County QL2 2017 WA3 LAS. (2019). U.S. Geological Survey. https://nationalmap.gov/3DEP/

Westerling, A. L., Hidalgo, H. G., Cayan, D. R., & Swetnam, T. W. (2006). Warming and earlier spring increase western U.S. forest wildfire activity. *Science*, *313*(5789), 940–943. https://doi.org/10.1126/science.1128834

Vukomanovic, J., Singh, K. K., Petrasova, A., & Vogler, J. B. (2018). Not seeing the forest for the trees: Modeling exurban viewscapes with LiDAR. *Landscape and Urban Planning*, *170*(November 2017), 169–176. https://doi.org/10.1016/j.landurbplan.2017.10.010

Yu, S., Yu, B., Song, W., Wu, B., Zhou, J., Huang, Y., Wu, J., Zhao, F., & Mao, W. (2016). View-based greenery: A three-dimensional assessment of city buildings' green visibility using Floor Green View Index. *Landscape and Urban Planning*, *152*, 13–26. https://doi.org/10.1016/j.landurbplan.2016.04.004

Yuan, C., Zhang, Y., & Liu, Z. (2015). A survey on technologies for automatic forest fire monitoring, detection, and fighting using unmanned aerial vehicles and remote sensing techniques. *Canadian Journal of Forest Research*, *45*(7), 783–792. https://doi.org/10.1139/cjfr-2014-0347